Degradation Behaviour of Natural Fibre Reinforced Starch-Based Composites under Different Environmental Conditions

Rosana Moriana*[,1,2], Emma Strömberg[1], Amparo Ribes[2] and Sigbritt Karlsson*[,1]

[1]*KTH Royal Institute of Technology, School of Chemical Science and Engineering, Fibre and Polymer Technology, Teknikringen 56–58, SE-10044, Stockholm, Sweden*
[2]*Materials Technology Institute (ITM), School of Design Engineering (ETSID), Polytechnic University of Valencia, Camino de Vera s/n, E-46022, Valencia, Spain*

Received January 31, 2014; Accepted April 08, 2014

ABSTRACT: The purpose of this work was to study the effect of hydrothermal, biological and photo degradation on natural fibres reinforced biodegradable starch-based (Mater-BiKE) composites to characterize the structural changes occurring under exposure to different environments. The composites water-uptake rate was hindered by the interfacial interactions between matrix and fibres. Thermal, structural and morphological analysis provided useful information about the irreversible changes in the properties of the composites caused by degradation in soil and photodegradation, and their synergetic effects. The effects due to the photo-oxidation and degradation in soil on the composites depended on the different chemical composition of each fibre. The composite with more hemicellulose and lignin in its formulation was more affected by both types of degradation, but still the end result properties were better than the ones shown for the degraded Mater-BiKE. The photo-oxidation of all the studied materials achieved enhanced degradation rate in soil. The Mater-BiKE/kenaf was shown to have the slowest water-uptake rate and better thermal properties once photo-oxidized, indicating better service life conditions. At the same time, the Mater-BiKE/kenaf was affected to a major extent by the synergetic effects of both photo-oxidation and soil burial test, showing a faster degradative rate and better disposal conditions.

KEYWORDS: Natural fibres, biodegradable polymers, composites, water absorption test, soil burial test, photodegradation test

1 INTRODUCTION

The huge volumes of plastic waste disposed of in landfills and the increasing problems posed by plastics waste management have stimulated the interest in developing degradable materials under non-controlled disposal conditions [1–3]. Some of these degradable materials show a lack of structural and dimensional stability for use in specific applications [4]. In this regard, the addition of natural fibres as reinforcements in biodegradable materials to improve their mechanical and thermal properties is a viable solution [5]. The design of composites based on biodegradable polymers from renewable resources and natural fibres opens up a broad range of sustainable opportunities such as: reducing the volume of synthetic plastic wastes and diminishing their negative environmental impact (contamination of soils and groundwater); reducing the demand of fossil resources; reducing the manufacturing energy and carbon dioxide neutrality. During the last years, the challenge has been to prepare natural fibre reinforced biodegradable polymer composites with a guaranteed suitable performance during their service life and which are still degradable after their disposal in soil. The study of the ageing behaviour of the composites under different environmental conditions, as well as the characterization of these reinforced composites, is a priority for assessing the potential applications and determining the life cycle of the materials. It is common to perform accelerated degradation tests for the simulation of ageing processes during the material's lifetime [6]. Hydrothermal tests for natural fibre composites have been proposed in order to assess water resistance [7, 8] and to predict

**Corresponding author*: rosana@kth.se, sigbritt.karlsson@his.se

DOI: 10.7569/JRM.2014.634103

the risk of microbial attack from humidity [9]. Photo-oxidation or weathering is another degradation test that has been used to evaluate the physical and chemical changes that occur in the composites due to solar and UV radiation [10, 11]. The biodegradation of different composites has also been evaluated by different methods, microbial growth tests [12] and soil burial conditions [13].

The purpose of this work was to study the hydrothermal, biological and photo degradation of natural fibres (kenaf and cotton) reinforced biodegradable polymer (Mater-Bi KE) composites through different accelerated tests: water absorption, soil burial and photo-oxidation. The water absorption test was proposed to assess the water resistance of the material during its service life. In addition, the samples were also submitted to radiation in order to study the degradation due to solar radiation and simulate the service life conditions. The photo-oxidized samples were also subjected to a soil burial test to model the further non-controlled disposal conditions in landfill. In previous works, the degradation process of Mater-Bi KE and Mater-Bi KE/cotton under soil burial conditions has been characterized in terms of thermal, structural and morphological changes [14]. A similar experimental methodology is proposed in this article in order to assess the synergetic effect of the photodegradation and degradation in soil processes on the chemical and physical properties of the materials. The influence of the chemical composition of each natural fibre on the degradation tests was also assessed and correlated with the resulting composite properties.

2 EXPERIMENTAL

2.1 Materials and Sample Preparation

A commercial thermoplastic starch-blend from Novamont Spa. (Italy), Mater-Bi KE03B1 (Mater-Bi KE) was used as polymeric matrix for preparing the reinforced composites. The commercial material, consisting of starch and ester components [15], was blended with kenaf and cotton fibres supplied by Yute Spain SL. The chemical composition of these two natural fibres are different; the cotton fibres have 90% cellulose and 2,3% hemicellulose, whereas the kenaf fibres present 57,6% cellulose, 22% hemicellulose and 11,8% lignin. Composites with 10% cotton and kenaf were prepared following the same methodology as previously published [15].

2.2 Experimental Accelerated Tests

2.2.1 Water Absorption Test

Water absorption experiments were performed following the ASTM D 570–98 standard [16]. Two specimens of each sample were submerged in distilled water at different temperatures: 29°C, 35°C and 42°C. The specimens were periodically removed from the water to be wheighted. The moisture uptake was calculated through Equation 1. The obtained absorption results were fitted following Equation 2 to assess the value of n and verify the diffusion behaviour of the material.

$$Mt = \frac{W_t - W_0}{W_0}(\%) \quad (1)$$

$$\frac{M_t}{M_\infty} = Kt^n \quad (2)$$

where $Mt\,(\%)$ is the moisture uptake, w_0 is the dry weight of the specimen, w_t is the specimen weight at time t of experiment, M_∞ is the moisture uptake at the equilibrium, and k and n are constants. The value of coefficient n can be classified in three different categories according to the relative mobility of the penetrant towards the polymer segments: Fickian diffusion ($n=0,5$) where the rate of diffusion is much less than that of the polymer segment mobility; Case II ($n=1$) and Super Case II ($n>1$) where the penetrant mobility is much greater than other relaxation processes, and finally; Non-Fickian diffusion ($0,5 < n < 1$) where the penetrant mobility and the polymer segment relaxation are comparable.

Once the diffusion model was assessed, the diffusion coefficient (D) was calculated from Equation 3, considering the initial uptake times (M_t/M_∞) ≤ 0, 5. Later it was verified that the diffusion process was activated by an increase in temperature, following an exponential Arrhenius-type relation with temperature (Equation 4). The activation energy was calculated from Equation 4.

$$\frac{M_t}{M_\infty} = \frac{4}{L}\cdot\left(\frac{D}{\pi}\right)^{0.5}\cdot t^{0.5} \quad (3)$$

$$D = D_0 \cdot exp\left(-\frac{Ea}{RT}\right) \quad (4)$$

Where L is the thickness and b represents the thickness dimensions of the sample, t is the immersion time, D_0 is the permeability index, Ea is the activation energy of the diffusion process, T is the temperature of the bath and R is the universal gas constant.

2.2.2 Photo-oxidation Test

Mater-Bi KE and reinforced composites were irradiated in an Atlas XLS+ Suntest with sunlight radiation

(280–700 nm). This radiation includes the spectrum of visible light and a part of the ultraviolet spectrum. The temperature of the black panel was 50°C. The samples were subjected to a constant radiation of 478W/m^2 during 1970 h, which renders a total radiation of 3390 MJ/m^2. The hours of radiation exposure can be converted into actual solar radiation by taking as a reference the minimum (2104 MJ/m^2) and maximum (7920 MJ/m^2) values for the annual solar radiation published by the European Commission [17]. The experimental total radiation is equivalent to 16 months of outdoor exposure in the less irradiated European areas such as northern Sweden. However, the same total radiation only simulates 5 months of solar radiation in the sunniest European countries such as Spain.

2.2.3 *Degradation in Soil Test*

According to the DIN 53739 international norm [18], samples were buried in active soil contained in plastic rectangular boxes. Two different sets of samples were buried: all the photo-oxidized samples and the non-irradiated Mater-Bi KE/kenaf samples. The soil burial test was carried out over 330 days, controlling the humidity, pH and temperature of the soil. Samples were taken out after different periods of time. Once removed, samples were washed with a soap solution in order to stop the degradation process.

2.3 Characterisation Techniques

2.3.1 *Thermogravimetric Measurements*

Thermogravimetric measurements were performed using a Mettler Toledo TGA/SDTA 851 thermogravimetric analyzer. Dynamic measurements were carried out from 25 to 750°C, at different heating rates from 3 to 20 °C/min under Argon atmosphere with a flow rate of 200 mL/min. The initial sample mass was between 8–9 mg. The onset and temperature peak of each thermal decomposition process was assessed as an indication of the thermal stability of each sample. The measurements were performed at least four times; the average and the average deviation from these data were considered as representative.

2.3.2 *Thermal Degradation Kinetics*

An integrated methodology that includes the Kissinger [19], Coats-Redfern [20] and Criado [21] methods was proposed to obtain the kinetic triplet (*Ea*, *A* and $f(\alpha)$) of the materials in previous studies [14, 15].

Among the assessed kinetic parameters, the *Ea* is chosen in this work as the most sensitive parameter to study the changes due to the degradation.

2.3.3 *Fourier Transform Infrared Spectrometry (FTIR) measurements*

The FTIR spectra were recorded at room temperature in a FTIR spectrometer Spectrum 2000 from Perkin Elmer (Wellesley, MA), equipped with a Golden Gate single-reflection accessory for attenuated total reflection measurements. Each spectrum was obtained by the performance of 32 scans between 4000–600 cm^{-1} at intervals of 1cm^{-1}. The FTIR spectra were smoothed and fitted by an automatic baseline correction by OMNIC 7.0 software. The measurements were performed seven times and the average deviations were considered for the calculus. The coefficient between the carbonyl groups (C=O) and (C-O-C) was proposed to study the degradation state of the pure Mater-Bi KE and corresponding reinforced composites.

2.3.4 *Scanning Electron Microscopy (SEM) Analysis*

SEM micrographs were obtained from cryogenic sectioned samples after sputtering with gold/palladium, using a JEOL JSM-5400 scanning electron microscope (JEOL Ltd., Japan).

3 RESULTS AND DISCUSSION

3.1 Water Absorption Test

Figure 1a shows the percentage of water absorbed as a function of the immersion time for Mater-Bi KE at different immersion temperatures (29, 35 and 42°C). The water uptake values increase as a function of the immersion temperature. However, Mater-Bi KE absorbs less than 1% of water and needs more than 25 hours to reach the maximum moisture uptake under any of the proposed immersion temperatures. The water uptake of the reinforced composites was also studied and compared with the obtained values for the Mater-Bi KE. The results presented in Figure 1b show higher water uptake values for the reinforced composites than for the Mater-Bi KE at 35°C. Similar patterns were obtained for the other temperatures, but are not presented for the sake of clarity. Table 1 summarizes the moisture uptake at the equilibrium (*Ms*) and the saturation time (*ts*) calculated from the absorption curves. In general, reinforced composites display higher *Ms* and longer *ts* than Mater-Bi KE. The hydrophilic character of the natural fibres is responsible for the higher values of *Ms* for the reinforced composites compared to Mater-Bi KE [4]. Hemicellulose is the most hydrophilic component in the natural fibre, so as expected, reinforced Mater-Bi KE/kenaf composites show higher *Ms* than the reinforced Mater-Bi KE/cotton composites.

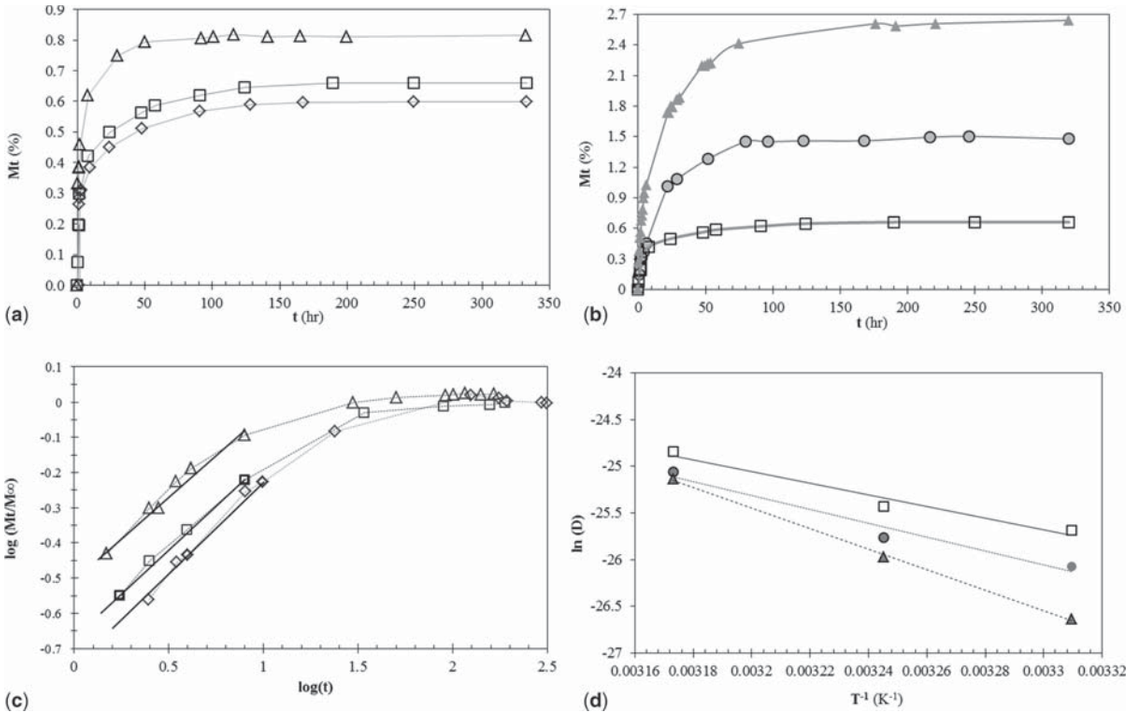

Figure 1 Water absorption analysis: **(a)** Absorption curves of Mater-Bi KE at (◊) 29°C, (□) 35°C and (Δ) 42°C, and **(b)** absorption curves of (□) Mater-Bi KE, (•) Mater-Bi KE/cotton, and (▲) Mater-Bi KE/kenaf at 35°C. **(c)** Log Mt/M∞ vs log (t) of Mater-Bi KE at (◊) 29°C, (□) 35°C and (Δ) 42°C to obtain n and k parameters. **(d)** Arrhenius dependence of the diffusion coefficient with temperature for (□) Mater-Bi KE, (•) Mater-Bi KE/cotton, and (▲) Mater-Bi KE/kenaf.

Table 1. Moisture uptake at equilibrium (Ms), saturation time (ts) and diffusion case selection parameters for Mater-Bi KE and its reinforced composites.

	29°C				35°C				42°C			
	M_s (%)	ts (h)	n	k (min^{-2})	M_s (%)	ts (h)	n	k (min^{-2})	M_s (%)	ts (h)	n	k (min^{-2})
Mater-Bi KE	0.60	44.9	0.46	0.21	0.70	34.5	0.51	0.21	0.80	25.0	0.48	0.29
Mater-Bi KE/cotton	1.10	83.2	0.42	0.18	1.40	69.5	0.48	0.14	1.80	37.3	0.49	0.30
Mater-Bi KE/kenaf	2.50	134.0	0.44	0.13	2.70	108.5	0.56	0.15	3.40	80.3	0.43	0.27

Figure 1c displays the assessment of the diffusion mechanism and kinetics for Mater-Bi KE at different immersion times according to Fick's theory. Table 1 also summarises the values of the parameters *n* and *k*. From the *n*-values it can be concluded that the diffusivity of all the studied materials at the different immersion temperatures follows Fickian behaviour. Applying Equation 3, the diffusion coefficient (D) is assessed from the experimental data (Table 2). As was expected, D increases as a function of the experimental temperature for all the studied materials. The reinforced composites absorb more water in the structure than the Mater-Bi KE; contrarily, the D value of the pure matrix was higher than the respective D value for the reinforced composites. Therefore, the presence of natural fibres contributes to slow down the diffusion mechanisms in the Mater-Bi KE due to the improved natural fibre/matrix interactions in the reinforced composites. Espert

et al. [5] stated that with better adhesion between matrix and fibres, the rate of the diffusion processes decreases since there are fewer gaps in the interfacial region and also because more hydrophilic groups from the matrix are blocked by the natural fibres.

Figure 1d displays the increase of D values as a function of the immersion temperature, showing the diffusion processes are activated by an increase in temperature following the Arrhenius equation. The *Ea* of each diffusional process was calculated from the pendent of these lines and are summarised in Table 2. The fibres incorporation into reinforced composites leads to an increase in the *Ea*, indicating that water uptake is hindered by the strong interfacial interactions between fibres and matrix [6]. Mater-Bi KE/kenaf exhibited the highest activation energies, probably due to the higher presence of hemicellulose and lignin in its composition that enables strong interactions between these fibres with the polymeric matrix [15]. These results are in accordance with the better thermal stability and mechanical properties assessed in a previous work [15] for the Mater-Bi KE/kenaf in comparison with the Mater-Bi KE/cotton.

Table 2 Diffusion coefficient (D) and activation energy (Ea) for Mater-Bi KE and corresponding reinforced composites at different experimental temperature.

	Diffusion coefficient . 10^{12} (m^2/s)			**Ea**
	29°C	**35°C**	**42°C**	**(kJ/mol)**
Mater-Bi KE	6.97	9.00	16.20	52
Mater-BiKE/ cotton	4.76	6.48	13.16	62
Mater-Bi KE/ kenaf	2.83	5.46	12.06	92

3.2 Photo-oxidation Tests

As already shown in previous works [22, 23], thermogravimetric analysis (TGA) can provide useful information about the irreversible changes in the properties of polymers caused by different degradation conditions. Presented in Figure 2 is a comparison

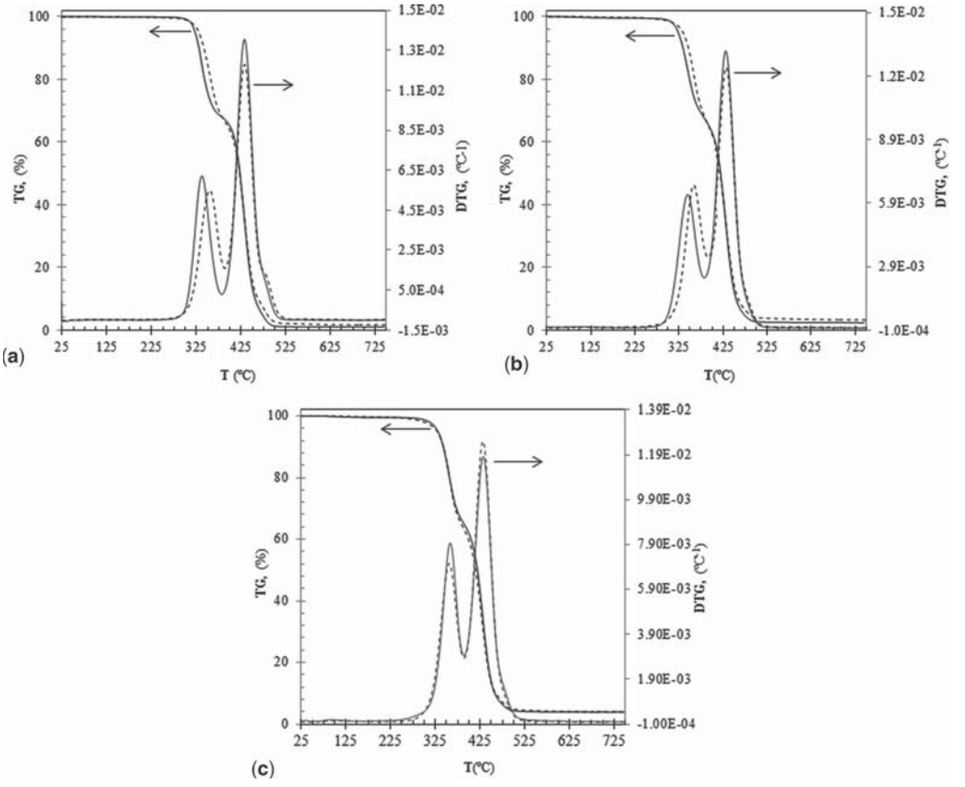

Figure 2 TG and DTG curves of: **(a)** (—) Mater-Bi KE and (---) photo-oxidized Mater-Bi KE; **(b)** (—) Mater-Bi KE/cotton and (---) photo-oxidized Mater-Bi KE/cotton; and **(c)** (—) Mater-Bi KE/kenaf and (---) photo-oxidized Mater-Bi KE/kenaf.

of the thermogravimetric (TG) and derivative thermogravimetric (DTG) curves of the photo-oxidized samples with the respective non-irradiated samples. As it was stated [15], the DTG curve of Mater-Bi KE presents two main mass-loss regions: the first one was related to the thermal decomposition of the starch and the second one to the synthetic polyester component. The photo-oxidation does not induce extensive changes in the shape of the Mater-Bi KE curves. However, the onset and temperature peak of the starch region is displaced to higher temperatures (DT=12°C), whereas the second mass-loss region associated with the polyester component is not significantly affected by the solar radiation. The reinforced composites were also subjected to the photo-oxidation test. Comparing the photo-oxidized reinforced composites with the respective non-irradiated samples differential effects are observed in the first thermal decomposition region depending on the added fibre. Similar to the Mater-Bi KE, the photo-oxidation induces an enhancement of 12°C in the onset and maximum temperature peak associated with the first decomposition peak in the Mater-Bi KE/cotton. However, in the Mater-Bi KE/kenaf the thermal stability is not altered due to the irradiation. This different behaviour of each reinforced composite may be attributed to the chemical composition of the natural fibre. It is known that hemicelluloses are much more susceptible to UV degradation than cellulose [24]. For this reason, the major content of hemicellulose in Mater-Bi KE/kenaf could alter the thermal stability trend showed for the Mater-Bi KE and Mater-Bi KE/cotton due to the photo-oxidation. On the other hand, the resulting thermal stability is slightly higher in the photo-oxidized reinforced composites than in the photo-oxidized Mater-Bi KE. This fact indicates the reinforced composites are more thermally stable than the pure polymeric matrix once photo-oxidized.

In order to analyse the thermogravimetric results in more detail and assess the kinetics involved in the degradation processes, the *Ea* of each thermal decomposition region was calculated. The *Ea* values related to the first thermal decomposition region (*Ea1*) and the *Ea* values of the second thermal decomposition region (*Ea2*) of the photo-oxidized Mater-Bi KE were assessed and the results were compared to the ones obtained for the non-irradiated samples (Figure 3a and 3b). Photo-oxidation enhances the *Ea* values of both components of Mater-Bi KE. This fact together with the enhancement at the onset may indicate crosslinking reactions in the Mater-Bi KE due to the photo-oxidation. However, when the *Ea* values of the photo-oxidized reinforced composites are compared with those calculated for the non-irradiated composites,

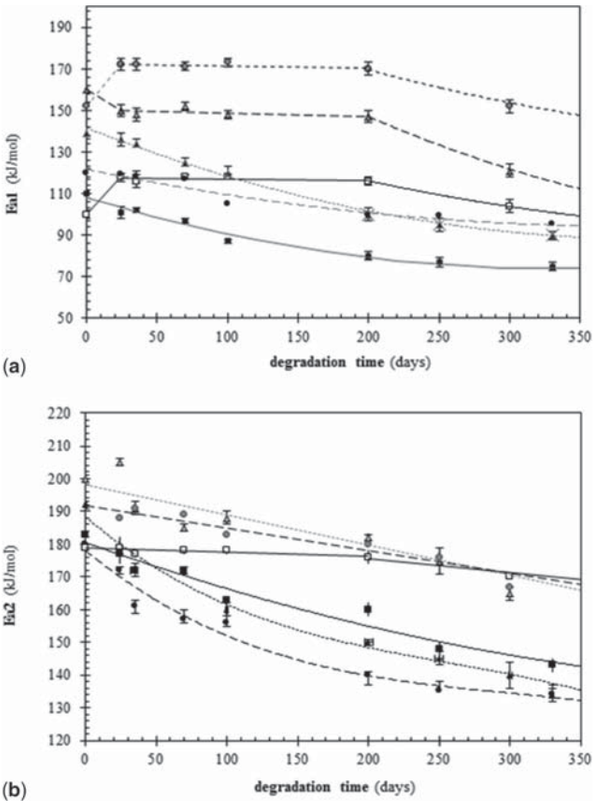

Figure 3 Representation of **(a)** Ea1 and **(b)** Ea2 as a function of the degradation time in soil for the: (□) Mater-Bi KE, (●) Mater-Bi KE/cotton, (▲) Mater-Bi KE/kenaf, (■) photo-oxidized Mater-Bi KE, (▲) photo-oxidized Mater-Bi KE/cotton and (•) photo-oxidized Mater-Bi KE/kenaf.

different behaviours are displayed; Mater-Bi KE/cotton shows a decrease in the *Ea2* values related to the synthetic component, whereas the presence of kenaf fibres resulted in a decrease of the *Ea* values of both thermal decomposition processes. The higher content of hemicelluloses and lignin in the Mater-Bi KE/kenaf may be responsible for this decrease in the *Ea* values. Therefore, these results indicate the major susceptibility of the Mater-Bi KE/kenaf to the effect of the irradiation. However, among all the photo-oxidized materials, Mater-Bi KE/kenaf is the one that shows the best thermal properties. The interactions of the Mater-Bi KE and kenaf fibres [15] resulted in a reinforced composite stable enough to show the best resulting thermal properties even after being affected to a major extent by photo-oxidation.

The FTIR analysis was performed in order to assess and verify the chemical structure changes due to the solar radiation. The FTIR spectra of photo-oxidized Mater-Bi KE showed a slight increase in the peak at

1089 cm^{-1} attributed to the stretching of C-O-C group in the glycosidic bonds (Figure 4). At the same time, a decrease in the OH and CH_2 group was established. Bajer *et al.* [25] stated that in the photochemical reactions of the polysaccharides the destruction of existing groups and formation of new carbonyl groups take place simultaneously, forming crosslinking. Comparing the photo-oxidized composites with the respective non-irradiated materials, different behaviours are observed depending on the type of natural fibre. A slight increase in the peak related to the stretching of C-O-C group in the glycosidic bonds was observed for photo-oxidized Mater-Bi KE/cotton composites, similar to Mater-Bi KE. However, the presence of kenaf fibres resulted in a decrease of this peak. Again, the presence of kenaf fibres seems to induce the chemical structure changes due to the effect of photo-oxidation of the Mater-Bi KE. This change could involve chain-scission reactions due to the highest content of hemicellulose and lignin in the Mater-Bi KE/kenaf composites.

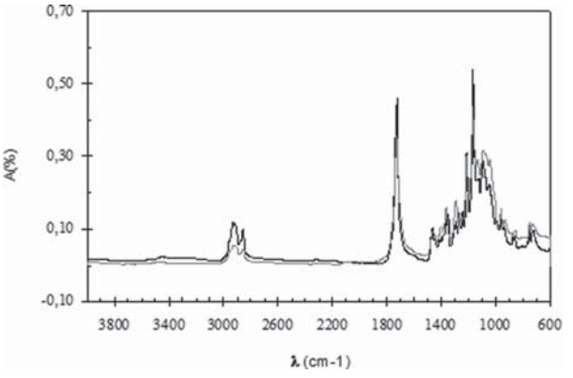

Figure 4 FTIR spectra of Mater-Bi KE (black curve) and photo-oxidized Mater-Bi KE (gray curve).

Finally, the possible morphological changes in Mater-Bi KE and the reinforced composites due to the photodegradation tests were evaluated. The cross-sections of the non-irradiated materials which are not shown in this study are similar to those images of the photodegraded samples in Figure 5. Therefore, solar

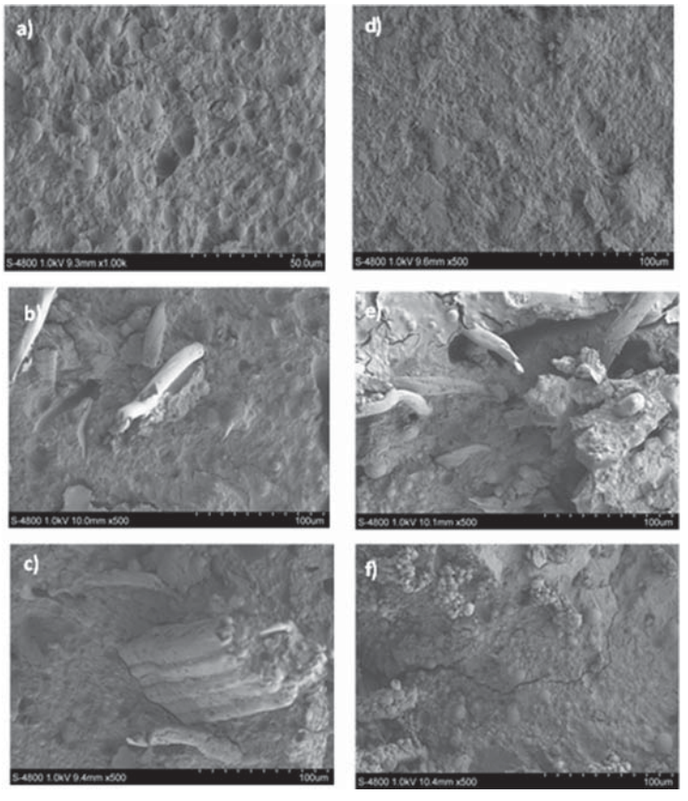

Figure 5 Micrographs of photo-oxidized samples: **(a)** Mater-Bi KE, **(b)** Mater-Bi KE/cotton and **(c)** Mater-Bi KE/kenaf. Micrographs of photo-oxidized samples subjected to soil burial test during 330 days: **(d)** Mater-Bi KE, **(e)** Mater-Bi KE/cotton and **(f)** Mater-Bi KE/kenaf.

radiation does not induce any significant morphological changes in the materials.

3.3 Degradation of Photo-oxidized Samples in Soil

The photo-oxidized samples were subjected to a soil burial test to model the further non-controlled disposal conditions in landfill. The Mater-Bi KE and the reinforced composites were characterised in terms of thermal, structural and morphological properties and compared with the samples only subjected to degradation in soil to evaluate the synergetic effect of both photo-oxidation and degradation in soil. When photo-oxidized Mater-Bi KE was subjected to degradation in soil, a decreasing trend in the onset was observed for both components as a function of the soil burial test (Table 3). The degradation in soil of non-irradiated Mater-Bi KE was assessed in previous studies [14] and the decreasing trend of the onset values was found from 200 days of degradation in soil. Therefore, preceding photo-oxidation seems to enhance the degradation rate of both components of pure Mater-Bi KE, already reducing thermal stability from the start of the degradation in the soil process. The TG and DTG curves of the non-irradiated Mater-Bi KE/cotton [14] and Mater-Bi KE/kenaf at different degradation times in soil were compared with the respective photo-oxidized and soil-degraded samples (Table 4–5). As it was observed for Mater-Bi KE, both Mater-Bi KE/kenaf and Mater-Bi KE/cotton showed a decreasing onset trend over 200 days of degradation. However, when the photo-oxidized reinforced composites were subjected to soil burial test a decreasing trend in the onset as a function of the soil burial test was determined for both thermal decomposition regions. The degradation rate during the soil burial tests for the photo-oxidized reinforced Mater-Bi KE/cotton composite was similar to that of the photo-oxidized Mater-Bi KE. However, for the photo-oxidized reinforced Mater-Bi KE/kenaf, the degradation rate of both thermal decomposition processes was higher. Thus the synergetic effect of the photo-oxidation and degradation in soil is much more pronounced for the materials containing kenaf compared to materials reinforced with cotton fibres.

In Figure 3a-b a comparison of the *Ea* values of the photo-oxidized and non-irradiated Mater-Bi KE samples as a function of the degradation in soil time is presented. The *Ea* values related to both thermal decomposition regions show a decreasing trend as a function of the soil burial test. Photo-oxidation altered the trend of the *Ea1* and *Ea2* values for the Mater-Bi KE as a result of the soil burial test, indicating an enhancement of the degradative rate of both components. The second thermal decomposition process related with synthetic component was most affected by the soil burial test once photo-oxidized (with a $\Delta Ea2$ of 39 kJ/mol). The synergetic effect of both degradation mechanisms on the deterioration of Mater-Bi KE resulted in lower *Ea1* and *Ea2* values at 330 days, indicating a more damaged material. Similar changes due to the photo-oxidation process were observed for the degradation of reinforced composites in soil and decreasing values of the *Ea* of both thermal decomposition processes were determined. However, a greater decrease of the *Ea* values for Mater-Bi KE/kenaf as a function of

Table 3 Thermogravimetric parameters of photo-oxidized Mater-Bi KE samples subjected to soil burial test.

	First Thermal Decomposition Process			Second Thermal Decomposition Process			Residue
Degradation Time (days)	Onset1 (°C)	Weight Loss 1 (%)	T peak1 (°C)	Onset2 (°C)	Weight Loss 2 (%)	T peak2 (°C)	Weight (%)
0	332.4±0.5	33.5±0.5	353.8±1.0	413.0±1.0	63.3±0.5	432.4±0.5	1.9±0.5
24	331.4±0.7	32.2±0.5	354.1±1.5	414.0±1.1	63.0±1.0	432.5±0.8	1.5±0.5
40	330.9±1.0	33.8±0.5	354.3±1.5	411.9±1.0	64.5±0.5	432.5±0.8	1.6±0.5
70	322.5±0.7	32.5±0.5	348.0±0.5	409.0±1.0	65.0±0.3	427.6±0.4	1.9±0.3
100	319.5±0.9	34.4±0.3	346.4±2.5	409.0±1.5	60.2±0.5	427.0±0.5	4.9±0.6
200	317.5±0.5	31.4±0.7	343.4±2.0	407.0±1.5	59.2±0.9	423.0±0.5	5.3±0.3
250	315.9±0.9	30.4±0.3	340.4±1.0	404.0±1.5	60.2±0.5	422.1±0.5	5.9±0.5
330	313.9±0.9	30.4±0.3	339.4±1.0	402.0±1.5	60.2±0.5	420.1±0.5	6.9±0.5

Table 4 Thermogravimetric parameters for Mater-Bi KE/kenaf and photo-oxidized Mater-Bi KE/kenaf as a function of the degradation in soil process.

	Mater-Bi KE/kenaf composite							Photo-oxidized Mater-Bi KE/kenaf composite						
	First Thermal Decomposition Process			Second Thermal Decomposition Process			Residue	First Thermal Decomposition Process			Second Thermal Decomposition Process			Residue
Degradation Time (days)	Onset1 (°C)	Weight Loss1 (%)	T peak1 (°C)	Onset2 (°C)	Weight Loss2 (%)	T peak2 (°C)	Weight (%)	Onset1 (°C)	Weight Loss1 (%)	T peak1 (°C)	Onset2 (°C)	Weight Loss2 (%)	T peak2 (°C)	Weight (%)
0	333.5±0.4	35.1±1.0	356.3±0.3	415.7±1.2	60.0±1.0	432.3±0.6	4.3±0.3	339.5±0.4	33.7±0.9	358.6±0.9	415.7±1.2	60.0±1.1	432.1±0.9	2.7±0.9
24	339.3±1.0	35.9±0.3	360.8±2.0	417.6±1.3	58.9±1.2	434.6±1.5	4.8±0.5	339.3±1.0	36.2±0.9	356.5±0.3	415.6±1.3	60.4±0.9	432.5±0.3	4.1±0.5
40	340.3±0.5	36.5±0.2	361.3±0.7	417.9±0.1	57.8±0.5	434.9±0.4	5.8±0.7	340.3±0.5	35.7±0.3	358.0±0.9	413.9±0.1	59.7±0.3	430.3±1.8	3.8±0.3
70	338.3±0.7	37.8±1.0	359.6±0.6	415.9±0.9	54.4±0.5	434.5±0.3	6.8±0.4	335.3±0.7	36.3±0.3	353.2±0.5	412.9±0.9	59.6±0.3	427.1±0.3	4.5±0.3
100	339.9±0.7	37.8±1.0	357.6±0.6	414.8±0.5	53.0±3.3	433.0±0.3	7.2±0.3	330.9±0.7	35.9±0.3	349.2±0.5	410.8±0.5	59.3±0.3	426.5±0.9	3.9±0.9
200	338.2±1.5	38.6±0.8	357.8±0.8	414.8±0.6	52.9±1.4	431.8±0.6	7.3±0.6	328.2±1.5	37.6±0.8	347.8±0.8	404.8±0.6	58.9±1.4	421.3±1.0	5.3±0.8
250	320.7±1.0	39.5±0.6	352.3±3.8	413.5±0.9	49.7±1.0	429.5±0.4	8.3±1.0	321.7±2.0	40.5±0.6	341.3±2.0	400.5±0.9	53.9±1.0	418.5±0.4	6.1±1.0
330	321.7±1.0	37.5±0.6	351.3±3.8	406.5±0.9	50.7±1.0	427.5±0.4	9.3±1.0	316.7±1.0	39.0±0.6	337.3±1.8	399.5±0.9	53.0±1.0	417.9±0.4	8.3±1.1

DOI: 10.7569/JRM.2014.634103

Table 5 Thermogravimetric parameters for Mater-Bi KE/cotton and photo-oxidized Mater-Bi KE/cotton as a function of the degradation in soil process.

	Mater-Bi KE/cotton composite							Photo-oxidized Mater-Bi KE/cotton composite						
	First Thermal Decomposition Process			Second Thermal Decomposition Process			Residue	First Thermal Decomposition Process			Second Thermal Decomposition Process			Residue
Degradation Time (days)	Onset1 (°C)	Weight Loss1 (%)	T peak1 (°C)	Onset2 (°C)	Weight Loss2 (%)	T peak2 (°C)	Weight (%)	Onset1 (°C)	Weight Loss1 (%)	T peak1 (°C)	Onset2 (°C)	Weight Loss2 (%)	T peak2 (°C)	Weight (%)
0	325.5±0.9	33.1±0.5	344.3±0.6	415.2±0.9	65.0±0.6	433.5±0.5	2.3±0.4	336.5±0.9	34.3±0.3	355.7±1.2	413.0±1.0	65.0±0.6	432.2±0.3	1.6±0.8
24	336.0±0.9	34.1±0.1	357.0±0.3	418.2±0.7	62.7±0.1	435.7±0.5	4.5±0.1	336.0±0.9	34.4±0.3	355.0±0.3	415.2±0.7	65.7±0.1	432.3±0.3	3.1±0.3
40	336.3±0.3	33.5±0.2	359.0±0.5	417.7±0.1	61.5±1.2	435.0±0.1	4.3±1.5	336.3±0.3	34.2±0.3	354.4±0.3	414.7±0.1	61.5±1.2	432.4±0.3	3.1±0.5
70	334.3±0.6	33.5±0.4	357.2±1.0	415.0±0.4	61.3±0.5	432.2±0.3	4.6±0.4	329.3±0.6	34.7±0.3	346.4±0.5	410.0±0.4	61.3±0.5	427.9±0.3	3.6±0.9
100	334.9±1.0	33.9±0.9	353.9±1.0	413.8±0.2	59.3±1.3	431.9±0.1	4.8±0.2	327.9±1.0	34.0±0.3	346.0±0.9	411.8±0.2	59.3±1.3	427.3±0.5	3.8±0.5
200	335.7±0.2	33.1±0.2	356.3±0.6	414.8±0.3	59.4±0.5	433.3±0.4	6.0±0.4	325.7±0.2	32.1±0.2	344.3±0.6	408.8±0.3	59.4±0.5	425.3±0.4	5.0±0.6
250	334.0±0.4	33.8±1.0	354.0±1.6	414.0±0.7	57.6±2.3	430.9±0.6	6.4±0.8	323.7±1.4	31.8±1.0	342.0±2.6	406.9±0.7	57.6±2.3	424.3±0.6	5.9±0.8
330	325.7±1.4	33.8±1.0	346.0±2.6	407.2±0.7	57.6±2.3	427.3±0.6	6.4±0.8	321.7±1.4	32.8±1.0	339.0±1.6	402.5±0.7	59.6±2.3	420.3±0.6	7.0±0.8

Table 6 $I_{C=O}/I_{C-O-C}$ of the non-irradiated and photo-oxidized samples as a function of the degradation in soil process.

	$I_{C=O}/I_{C-O-C}$					
Degradation Time (days)	**Mater-Bi KE**	**Mater-Bi KE/ cotton**	**Mater-Bi KE/ kenaf**	**Photo-oxidized Mater-Bi KE**	**Photo-oxidized Mater-Bi KE/ cotton**	**Photo-oxidized Mater-Bi KE/ kenaf**
0	1.76	1.73	1.52	1.50	1.40	1.60
100	1.34	0.99	0.70	1.00	0.70	0.85
200	1.34	0.98	0.65	0.85	0.65	0.73
250	1.20	0.97	0.63	0.55	0.60	0.60
330	1.00	0.96	0.61	0.50	0.55	0.48

the degradation time ($\Delta Ea1$=49 kJ/mol; $\Delta Ea2$=52 kJ/mol) was observed compared to Mater-Bi KE/cotton ($\Delta Ea1$=24 kJ/mol; $\Delta Ea2$=40 kJ/mol). These differences may be due to the chemical composition of each natural fibre; the major amount of hemicellulose and lignin in the kenaf fibres enhanced the synergetic effects of photo-oxidation and soil burial test for Mater-Bi KE.

The FTIR spectra of the photo-oxidized samples and samples degraded in soil were analysed. Two bands were selected in order to monitor the degradation changes: the band placed at 1733 cm^{-1} (-C=O stretch) was selected to monitor the degradation of the synthetic component of Mater-Bi KE; the band at 1089 cm^{-1} (C-O-C stretch) was chosen to monitor starch degradation in Mater-Bi KE. Table 6 summarises the $I_{C=O}/I_{C-O-C}$ ratio values of the photo-oxidized Mater-Bi KE samples buried for different degradation times. The $I_{C=O}/I_{C-O-C}$ ratio values of the non-irradiated Mater-Bi KE, previously published [14], were compared with the photo-oxidized Mater-Bi KE. Preceding photo-oxidation increased the degradative rate of polyester component with respect to the starch as a function of the soil burial time. Similar results were observed for the photo-oxidized reinforced composites as a function of the soil burial time (Table 6). Preceding photo-oxidation enhanced the degradative rate of polyester component with respect to the starch as a function of the soil burial time for both reinforced composites, but was more pronounced for Mater-Bi KE/kenaf. The synergetic effect of photo-oxidation and degradation in soil is higher for Mater-Bi KE/kenaf due to the major amount of hemicellulose and lignin in its formulation

Scanning electron microscopy was used to examine the possible morphological changes in pure Mater-Bi KE and the reinforced composites due to the synergetic effects of both photo-oxidation and soil burial tests. The photo-oxidized and degraded reinforced composites showed the emergence of cracks and cavities (Figure 5). The results indicated a more damaged structure of the materials compared to the respective non-irradiated reinforced composites subjected to degradation in soil over 330 days.

4 CONCLUSIONS

The hydrothermal behaviour was assessed in terms of water absorption capacity, saturation times and water diffusion kinetics. The presence of natural fibres in the reinforced composites was responsible for higher saturation capacity and lower saturation time. The water absorption process of the polymeric matrix and the reinforced composites was found to follow the kinetics and mechanisms described by Fick's theory. In addition, the diffusivity coefficient value was greater for the polymeric matrix than for the reinforced composites, indicating a prevention of water uptake due to the interactions between the polymeric matrix and the natural fibres. The diffusivity coefficient showed Arrhenius dependence with the temperature, and the activation energy for all the reinforced composites was higher than for the pure polymer. It was concluded that although the natural fibres add higher hydrophilic character to the samples, the water uptake process is hindered by the interfacial interactions between matrix and fibres.

Thermal, structural and morphological analysis provided useful information about the irreversible chemical and physical changes caused by degradation in soil, photo-degradation and their synergetic effects on the reinforced composites. Photo-oxidation induces changes in the thermal and structural properties related to the starch component of the Mater-Bi KE due to crosslinking reactions. However, similar changes were not observed for the reinforced composites, indicating that the influence of photo-oxidation is dependent on the chemical composition of the natural fibres. The photo-oxidized reinforced composites showed better thermal and kinetics properties than the photo-oxidized pure Mater-Bi KE. Analysis of Mater-Bi KE/

kenaf showed the slowest diffusivity coefficient value and better thermal properties once the material was photo-oxidized, indicating a better service life performance. Solar radiation enhanced the degradation rate of all the materials buried in soil, where Mater-Bi KE/kenaf was most affected by the synergetic effects of both photo-oxidation and the soil burial test.

ACKNOWLEDGMENTS

The financial support given by KTH Royal Institute of Technology is gratefully acknowledged. The Spanish Ministry of Education is acknowledged for the concession of a pre-doctoral research position to Rosana Moriana through the FPI program.

REFERENCES

1. F. La Mantia, *Handbook of Plastics Recycling*, Rapra Technology, Shrewsbury, UK. (2002).
2. S.J. Huang, Polymer waste management: Biodegradation, incineration and recycling, in *Degradable Polymers, Recycling and Plastics Waste Management*, A.C. Albertsson and S.J. Huang, (Eds.), pp. 1–7, New York, Marcel Dekker. (1995).
3. M. Smits, *Polymer Products and Waste Management*, International Books, Utrecht, Germany. (1996).
4. A. Bismarck, S. Mishra, and T. Lampke, Plant fibers as reinforcement, in *Green Composites, in Natural Fibers, Biopolymers and Biocomposites*, A.K. Mohanty, M. Misra, and T.D. Drzal, (Eds.), pp. 37–109, Taylor & Francis, Boca Raton, Florida. (2005).
5. A.K. Mohanty, M. Misra, and G. Hinrichsen, Biofiber, biodegradable polymers and biocomposites: A review. *Macromol. Mater. Eng.* **276**, 1–4 (2000).
6. H. Bansa, Accelerated aging tests in conservation research: Some ideas for a future method. Restaurator 13, 114–137 (1992).
7. A. Espert, F. Vilaplana, and S. Karlsson, Comparison of water absorption in natural cellulosic fibres from wood and one-year crops in polypropylene composites and its influence on their mechanical properties. *Comp. A Appl. Sci. Manuf.* **35**, 1267–1276 (2004).
8. T. Kittikorn, E. Strömberg, M. Ek, and S. Karlsson, Comparison of water uptake as a function of surface modification of empty fruit brunch oil palm fibers in PP biocomposites. *BioResources* **8**, 2998–3017 (2013).
9. E. Strömberg and S. Karlsson, The Effect of biodegradation on surface and bulk property changes of polypropylene, recycled polypropylene and polylactide biocomposites. *Int. Biodeterior. Biodegrad.* **63**, 1045–1053 (2009).
10. F.G. Torres, O.H. Arroyo, C. Grande, and E. Esparza, Bio- and photo-degradation of natural fiber reinforced starch-based biocomposites. *Int. J. Polym. Mater.* **55**, 1115–1132 (2006).
11. R. Moriana-Torró, L. Contat-Rodrigo, L. Santonja Blasco, and A. Ribes-Greus, Thermogravimetric characterisation of photo-oxidized HDPE/Mater-Bi and LDPE/Mater-Bi blends buried in soil. *J. Appl. Polym. Sci.* **109**, 1177–1188 (2008).
12. T. Kittikorn, Tuning the long-term properties to control biodegradation by surface modifications of agricultural fibres in biocomposites, PhD Thesis ISSN: 1654–1081, KTH Royal Institute of Technology (2013).
13. L. Santonja-Blasco, R. Moriana, J.D. Badía, and A. Ribes-Greus, Thermal analysis applied to the characterization of degradation in soil of polylactide: I. Calorimetric and viscoelastic analyses. *Polym. Degrad. Stabil.* **95**, 2185–2191 (2010).
14. R. Moriana, S. Karlsson, and A. Ribes-Greus, Assesing the influence of cotton fibres on the degradation in soil of a thermoplastic starch-based biopolymer. *Polym. Compos.* **31**, 2102–2111 (2010).
15. R. Moriana, F. Vilaplana, S. Karlsson, and A. Ribes-Greus, Improved thermo-mechanical properties by the addition of natural fibres in starch-based sustainable biocomposites. *Compos. A Appl. Sci. Manuf.* **42**, 30–40 (2011).
16. Standard test method for water absorption of plastics, ASTM D570–98 (2010).
17. JRC-European Comission, Photovoltaic geographical information system, http://re.jrc.ec.europa.eu/pvgis/apps4/pvest.php (2005).
18. Testing of plastics; influence of fungi and bacteria; visual evaluation; change in mass or physical properties, DIN 53739 (1984).
19. H.E. Kissinger, Variation of peak temperature with heating rate in differential thermal analysis. *J. Res. Natl. Bur. Stand.* **57**, 217–221 (1956).
20. A.W. Coats and J.P. Redfern, Kinetics parameters from thermogravimetic data. *Nature* **201**, 68–69 (1964).
21. J. M. Criado, Kinetic Analysis of DTG data from master curves. *Thermochim. Acta* **24**, 186–189 (1978).
22. J.D. Badía, L. Santonja-Blasco, R. Moriana, and A. Ribes-Greus, Thermal analysis applied to the characterization of degradation in soil of polylactide: II. On the thermal stability and thermal decomposition kinetics. *Polym. Degrad. Stabil.* **95**, 2192–2199 (2010).
23. J.D. Badía, R. Moriana, L. Santonja-Blasco, and A. Ribes-Greus, A thermogravimetric approach to study the influence of biodegradation in soil test to poly(lactic acid). *Macromol. Symp.* **272**, 93–99 (2008).
24. W. Thielemans and R.P. Wool, Butyrated kraft lignin as compatibilizing agent for natural fiber reinforced thermoset composites. *Compos. A Appl. Sci. Manuf.* **35**, 327–338 (2004).
25. I. Kardas, W. Marcol, A. Niekraszewicz, M. Kucharska, D. Cienchanska, D. Wawro, J. Lewing-Kowalik, and A. Wlaszczuk, Utilization of biodegradable polymers for peripheral nerve reconstruction, in *Progress on Chemistry and Application of Chitin and its Derivatives*, M.M. Jaworska, (Ed.), pp. 159–167, Polish Chitin Society, Łódź. (2010).